Climate Change and Dynamics of Crop Yield Distribution

Fengxia Dong

Fengxia.dong@usda.gov

Research Agricultural Economist

Economics Research Service

U.S. Department of Agriculture

Xiaodong Du

Xdu23@wisc.edu

Professor

Department of Agricultural and Applied Economics

University of Wisconsin-Madison

Selected Paper prepared for presentation at the 2024 Agricultural & Applied Economics Association Annual Meeting, New Orleans, LA; July 28-30, 2024

Abstract

This study explores the dynamics of corn yield distribution and convergence at the county level in the United States. Stochastic transition kernels are estimated for relative county yields scaled by the national average across four sub-periods from 1955 to 2021. Unconditional transition kernels demonstrate the convergence of both relative yields and per-acre incomes, the latter of which include indemnity payments of crop insurance. When conditional on weather variables, specifically temperature and precipitation, the conditional transition kernels highlight the effects of climate change on the dynamics of crop yield distribution. These effects include a more significant reduction in the upper portion of the distribution compared to the lower part, leading to convergence towards the national average. The impact on crop income is evident in both the left tail and the level and probability of the mean.

Keywords: Climate change, contour plot, ergodic distribution, stochastic transition kernel, transition matrix, yield convergence.

JEL Classification: Q10, Q54, C14

1 Introduction

The distribution of crop yields has consistently been shaped by a range of factors, such as weather changes, technological advancements, and improvements in farm management. For example, hybrid corn seeds introduced in the early 20th century and genetically modified corn hybrids commercialized in the late 1990s have made significant contributions to increasing yields. These innovations have had a notable impact on various aspects of corn yield distribution, including the mean, variance, and skewness (Chavas and Shi, 2015; Griliches, 1957; Lusk et al., 2019; Shi et al., 2013). Weather conditions such as temperature and precipitation, along with farmers' adaptations to climate, including crop diversity and management practices, have been found to significantly affect crop yields and their spatial correlations (e.g., Falco and Chavas, 2008; Goodwin, 2001; Schlenker and Roberts, 2009; Tack and Holt, 2016).

Crop yield distribution and its influencing factors have been quantified using, for example, conditional quantile regression-type models (e.g., Barnwal and Kotani, 2013; Chavas et al., 2019; Ramsey, 2023; Sanglestsawai et al., 2014). Across countries and crops, a consistent finding is that the impact of weather or technology varies across quantiles of crop yield distribution and is not symmetric, with a larger impact on the lower tail compared to the upper tail of the yield distribution. Based on moment-based methods, studies in the literature document the asymmetry of input effects on yield distribution (Antle, 1983, 2010), and beneficial factors to crop production, such as fertilizer and precipitation, are found to make the yield distribution more negatively skewed (Du et al., 2012, 2015). Other empirical methods being applied include, for example, a normal mixed model (Tolhurst and Ker, 2015), parametric distribution function like the beta distribution (Nelson and Preckel, 1989; Ramirez, 1997), and nonparametric and semiparametric methods (Goodwin and Ker, 1998; Ker and Coble, 2003; Ker and Goodwin, 2000). One specific focus of these methods involves statistical properties of yield distribution such as nonnormality, left skewness, and kurtosis.

Income convergence across US states and counties, especially during the early period up to the 1990s, has been well documented in the growth-convergence literature (e.g., Barnwal and Kotani, 2013; Higgins et al., 2006). The typical empirical evidence supporting income convergence is the so-called unconditional β-convergence, where β refers to the coefficient of the initial income when regressing the average growth rate on it. The empirical strategy for estimating

distribution dynamics proposed in Quah (1993, 1996a,b, 1997) has been widely adopted to examine economic convergence and divergence. By imposing a first-order Markov structure, the approach estimates the corresponding transition kernel and steady-state distribution implied by that kernel to comprehensively understand the dynamics of the entire distribution. A recent example is found in Park and Shin (2023), which utilizes the distribution dynamics method to analyze the rising inequality in US county-level per capita income. This is the method we adopt in this study to understand the dynamics of county-level crop yield distribution and the convergence of relative yields over time.

Deviating from the existing crop yield literature, we normalize county-level corn yields by the national average in each sample year over the period of 1955-2021. This process allows us to shift our focus from trend yield to relative yields for exploring the unconditional and conditional dynamics of yield distribution changes. Specifically, we estimate the nonparametric stochastic transition kernel for each 20-year period to understand the distribution changes of corn yields. The analysis illustrates a clear trend of convergence of relative yields over time. To understand the reasons behind this phenomenon, we further estimate the transition kernels conditional on weather variables including growing degree days (GDD), overheating degree days (ODD), and precipitation over the same periods corresponding to unconditional kernels. The comparison between unconditional and conditional transition kernels indicates that climate change pulls down the relative yields at the upper part of the yield distribution at a much larger magnitude than those at the lower tail, leading to the observed convergence.

As the most important risk management tool in the current period, crop insurance insures crop revenue against yield and price drops. To examine the effect of crop insurance on per acre income (crop sales plus indemnity payment), we estimate the transition kernel of county-level per acre income distribution from 1997 to 2021, a period during which the adoption of crop insurance increased significantly, as a result of large increases in premium subsidies. The result indicates that indemnity payments, to some extent, dominate crop sales and completely remove the lower tail of the income distribution, leading to income convergence toward the national average.

The rest of the paper is organized as follows. In Section 2, we conduct preliminary analyses to understand the dynamics of crop yield distribution using box plots and discrete analysis

of distribution transition over time. Section 3 estimates the stochastic transition kernels for relative yields over sub-periods spanning from 1955 to 2021. The transition kernel for per-acre income distribution is then estimated and discussed for the period of 1997-2021. In Section 4, the impact of climate change on relative yield distribution is quantified, emphasizing its contribution to yield convergence. Section 5 concludes.

2 Data and Preliminary Analysis

In this study, we focus on the following 13 major corn-producing states: Illinois, Indiana, Iowa, Kansas, Michigan, Minnesota, Missouri, Nebraska, North Dakota, Ohio, Oklahoma, South Dakota, and Wisconsin. County-level yield records are collected from the database maintained by the National Agricultural Statistical Service (NASS) of the U.S. Department of Agriculture.[1]

We focus on four periods, 1955-1959 (P1), 1975-1979 (P2), 1997-2001 (P3), and 2017-2021 (P4), as marked by the vertical lines in Figure 1 to document the dynamic changes of corn yield distribution. Figure 1 presents the historical annual corn yields from 1886 to 2023. The sample period, spanning from 1955 to 2021, illustrates a dramatic improvement in yields, which increased almost linearly with only a few instances of sudden drops followed by subsequent recovery. Examining changes in yield distribution over a 20-year period insulates us from short-term weather and policy shocks, allowing us to focus on longer-term climate and technical changes. The estimations in the subsequent analyses are conducted based on the averages of five pairs between subperiods, such as 1955-1975, 1956-1976, 1957-1977, 1958-1978, and 1959-1979 for periods P1 and P2. This approach further eliminates the influence of temporary yearly variations. All selected subperiods exhibit stable yields without sudden changes likely induced by extreme weather events. The year 1955 marked the beginning of significant yield improvement driven by the widespread adoption of hybrid corn. The period of P2 occurred before, while P3 and P4 took place after the development and extensive adoption of genetically modified (GM) crops in the late 1990s. This development, especially the adoption of Bt Corn, significantly increased corn yields.

Figure 2 displays box plots of relative county yields in 1955, 1975, 1997, and 2017. The yields are calculated by dividing the individual county yields by the sample mean of each

[1]The data is available at: https://quickstats.nass.usda.gov/.

respective year. In each plot, the box represents the interquartile range (IQR), extending from the first quartile (25%) to the third quartile (75%) of the relative yields. The whiskers show the minimum and maximum values within a range of $1.5 \times IQR$. The individual dots outside the whiskers indicate outliers or extreme values of relative yields.

The box plots in Figure 2 illustrate several noteworthy patterns, including the following: (i) the interquartile range becomes smaller over time, indicating a tighter clustering and reduced variability of the middle 50% of relative yields. (ii) The median, represented by the horizontal bar in the plot, consistently decreases from 1955 to 1997. This suggests a shift in the middle value of yields closer to the national average, as reflected in the rising 25% quartiles and dropping 75% quartiles over time. (iii) There is an increasing number of counties with extremely poor yields relative to others. In summary, we observe a general trend of relative yield convergence over the sample period, while certain counties lag behind with significantly lower yields compared to others.

To understand the dynamics of crop yield distribution, we quantify transitions of specific parts of the yield distribution over time. Specifically, we consider five ranges (1 to 5) of county-level yield relative to the national average: [0,0.5], [0.5,0.75], [0.75,1],[1,1.25],[1.25,2].[2] For example, a value of 0.5 corresponds to being half of the national average, while a value of 1 means being equal to the national average. In each sub-period, we compute the transition matrix among ranges for five pairs of years. For example, to document the changes between P1 and P2, we calculate the transition matrices for the year pairs of 1955-1975, 1956-1976, 1957-1977, 1958-1978, using the first year (e.g., 1955) as the start year and the second year as the end year (e.g., 1975), and then take the average. The diagonal elements of the transition matrix indicate the tendency to stay in the same range over time. The results are shown in Table 1.

The three transition matrices between P1 and P2, P2 and P3, and P3 and P4 exhibit similar patterns. First, there are significant transitions from ranges below the national average, such as [0,0.5], [0.5,0.75], and [0.75,1], to higher ranges. For example, during the period from P1 to P2 (1955-1979), 30% of counties initially in range 1 (0-0.5) improved their yields, moving to range 2 (0.5-0.75) by the end, while 30% that began in range 2 moved up to range 3 (0.75-1).

[2]The maximum relative yield in all sample years is 1.63, so the last range covers all values above 1.25.

Additionally, 29% of counties in range 3 moved up to range 4 (1-1.25) over the period. This trend accelerated from the mid 1970's to the late 1990's (P2-P3), with corresponding upward movements of 43% ($1 \rightarrow 2$), 51% ($2 \rightarrow 3$), and 36% ($3 \rightarrow 4$). Although the upward trend slowed down in the more recent period of P3-P4 (1997-2021), it remains significant, with proportions of 41% ($1 \rightarrow 2$), 43% ($2 \rightarrow 3$), and 39% ($3 \rightarrow 4$), respectively.

Second, for the two highest ranges, [1,1.25] and [1.25,2], the most common transition across all sub-periods is a shift to the immediately adjacent lower range. For example, during the period of P1-P2, 28% of counties shifted from the range [1,1.25] to [0.75,1], while 40% in the highest range moved down to the range of [1,1.25]. This type of transition becomes more intensive in the later two sub-periods, especially for the highest range, with a transition proportion of 64% in P2-P3 and 61% in P3-P4. In summary, we observe a convergence of county-level relative yields of corn over time, as lower-yield counties catch up with others, moving closer to the national average, while higher-yield counties also shift toward the national average.

3 Unconditional Distribution Dynamics

In the preliminary analysis, we discretize the relative yield distribution into five ranges and count the observed transitions to describe distribution dynamics, as reported in Table 1. For continuous variables like crop yields, such discretization may distort distribution dynamics in significant ways (Quah, 1996b). The solution is to use a stochastic kernel to fully describe the distribution dynamics over time.

Building on existing literature (Park and Shin, 2023; Quah, 1996a, 1997), we employ a stochastic kernel to describe the evolution of the county-level yield distribution from $f_t(x)$ in year t to $f_{t+p}(y)$ in year $t+p$ ($p > 0$). Here, $f_t(\cdot)$ and $f_{t+p}(\cdot)$ represent the yield density functions. The stochastic kernel m_p over the period p is formulated as follows:

$$f_{t+p}(y) = \int_0^\infty m_p(y|x) f_t(x) dx,$$

where $m_p(y|x)$ is the conditional density of the yield y p periods ahead, given the value of x. It provides detailed information on intradistribution dynamics, including, for example, where

points in the distribution of f_t end up in f_{t+p}.

The stochastic kernel m_p is estimated non-parametrically in the following steps:[3] (i) Estimate the joint density of x and y, which represent the county yields in period t and $t+p$, respectively, using the Gaussian kernel function. (ii) Determine the marginal density of x by integrating the joined density obtained in step (i) with respect to y. (iii) Compute $m_p(y|x)$ by dividing the joint density from step (i) by the marginal density calculated in step (ii).

With the estimated transition kernel $m_p(y|x)$, the steady-state or ergodic distribution, denoted as f_∞, can be generated by repeatedly applying the kernel as follows:

$$f_\infty^{(k+1)} = \sum_{i=1}^{n} m_p(y|x_i) f_\infty^{(k)}(x_i), \text{ for } k = 0, 1, 2, \ldots, I.$$

In our case, we set the number of iteration, I, to 500. The starting point of the process is f_∞^0, which represents the predicted marginal density of y at the end year of the sample period.

Figure 3 presents the surface and contour plots of the estimated transition kernels over the subperiods of P1-P2 (panels a and b), P2-P3 (c and d), and P3-P4 (e and f). In simple terms, a stochastic kernel can be imagined as extending the number of ranges (or rows and columns of the transition matrix as reported in Table 1) to infinity. Starting from any point on the axis labeled "Relative yield at t_0" and extending in parallel to the axis labeled "Relative yield at t_0+20,"[4] the stochastic kernel represents a probability density function that describes transition probabilities or how the county-level yield distribution evolves over the period (Quah, 1996b). These transition probabilities are all positive and sum to 1.

If the surface mass is concentrated along the 45-degree diagonal, indicated by the black dashed line on the $x-y$ space, yields in the distribution remain unchanged from the initial level. When the mass is rotated counterclockwise away from the 45-degree diagonal, yield convergence occurs, meaning that high yield decreases, and low yields increases. The extend of convergence is indicated by the red solid line on the $x-y$ space, representing the predicted mean yield in the end year for each level of initial yield in the start year (Park and Shin, 2023). We observe yield convergence for all subperiods in the surface plots shown in Figure 3.

This is further illustrated in the corresponding contour plots shown in Figure 3. In each

[3]Please refer to Park and Shin (2023) for the details of the estimation.

[4]Please note that the length of a specific subperiod may vary and depends on the end year of the corresponding sample period.

contour plot, the vertical axis represents the relative yield at the beginning of the period (e.g., 1955 for P1-P2, 1975 for P2-P3, and 1997 for P3-P4), while the horizontal axis represents that for the end year (i.e., 1975 for P1-P2, 1997 for P2-P3, and 2017 for P3-P4). The 45-degree diagonal line and predicted end-year yields are also depicted. The red line crosses the 45-degree line from below at the level of national average, where relative yield is 1, indicating unconditional or absolute convergence (Park and Shin, 2023). For yields below the national average, convergence occurs in all subperiods, especially during the period of P2-P3 when the increase is most significant. For yields above the national average, convergence continues throughout the entire sample period, with an increasing shift toward 1. The speed of convergence near the cross point is determined by the slope of the red line. Notably, the convergence speed from above (higher than the national average) is similar across periods and is fastest when converging from below or catching up with lower yields over the period of 1975-1997 (P2-P3; panel d).

Figure 4 illustrates the ergodic distributions of subperiods (shown as black curves). The ergodic distribution represents the steady-state outcome obtained by repeatedly applying the estimated transition kernel to the predicted end-year marginal density in each subperiod, labeled as the "Start year" in the figure. In the 20-year period of P1-P2 (1955-1975; panel a), the ergodic density of relative yield is less evenly distributed, with thicker tails on the left and right sides but a lower peak compared to the start year in 1959. In the P2-P3 period (panel b) and P3-P4 period (panel c), the ergodic densities are quite similar to each other and to that of the start year, exhibiting a denser peak and a longer right tail compared to panel (a). This indicates that, in general, more counties experienced increasing yields over these periods, while yields converged toward the national average.

In the following, we conduct a similar exercise to understand the effect of crop insurance on farm income. We incorporate the indemnity payment for corn into the crop revenue. Specifically, county-level indemnity payments are aggregated across insurance plans and coverage levels,[5] and then converted to the per-acre indemnity payment by dividing the total acres of a specific county.

To make corn revenue comparable to insurance payments, we multiply the crop yields by

[5]County-level indemnity payments are available in the Summary of Business reports maintained by the Risk Management Agency (RMA) of the U.S. Department of Agriculture and can be downloaded from https://www.rma.usda.gov/Information-Tools/Summary-of-Business/State-County-Crop-Summary-of-Business.

the corn price as the larger of the insurance base price and harvest prices. The base price is the average February price, and the harvest price is the average October price of the December futures contract traded on the Chicago Mercantile Exchange. We focus on the period between P3 (1997-2001) and P4 (2017-2021) to document the distribution dynamics of county-level per-acre corn income, which is defined as the sum of corn revenue and indemnity payment per acre. This period is chosen primarily due to the higher participation in crop insurance compared to previous years.

The resulting surface plot, contour plot, and ergodic distribution are presented in Figure 5. Both the surface and contour plots show that the majority of the transition are concentrated around the value of 1 on the Period $t_0 + 20$ axis, almost entirely parallel to the Period t_0 axis. This suggests a convergence of the cross-section income distribution towards equality, although there are some deviations for the initial income in the range of (3,5). This convergence is further confirmed in the distribution plots, where both the distribution in 2021, labeled as the "Start year", and the ergodic distribution demonstrate a complete reduction of the lower tail and an extension of the right tail. This implies that crop insurance compensates counties with lower yields and higher income losses, while simultaneously adding income to other counties with relatively higher crop revenues.

4 Conditional Distribution Dynamics

To understand the impact of weather conditions or long-term climate change on the distribution of crop yields, we estimate distribution dynamics while controlling for these factors. This process involves two steps: (i) Estimating a linear regression model for crop yields by incorporating weather variables as controls after pooling samples from each subperiod (P1 to P4). (ii) Utilizing the regression residuals from step (i) to derive conditional distributions for each sample year and estimating the transition kernel using these conditional distributions.[6] To maintain consistency with the unconditional distribution, we apply the same set of years—namely P1, P2, P3, and P4—in the conditionals for estimation.

We begin our discussion by examining weather-related variables at the county level. Follow-

[6]We add the estimated intercept to the residuals since our goal is to remove only the weather related impact. Following that, we exclude negative residuals, which constitute at most 5% of the observations.

ing existing literature (e.g., Du et al., 2015; Gong et al., 2023), we construct three county-level weather variables—growing degree day (GDD), overheating degree days (ODD), and precipitation during the growing season (May to August)—for each sample year. GDD is measured as the sum of degrees in the range of [8°C, 32°C], which is beneficial for crop growth. On the other hand, ODD represents the cumulative degree days exceeding 32.22°C (Gong et al., 2023; Schlenker and Roberts, 2009), which can stress and harm crop growth. Precipitation is calculated by summing the total rainfall over the growing season. We utilize daily weather data provided by the National Oceanic and Atmospheric Administration (NOAA) for constructing the weather variables.[7]

The regression results of step (i) are reported in the upper panel of Table 2. Intercept increases over time, indicating the continuously improving trend in yield. The effects of three weather variables—GDD, ODD, and Precipitation—vary over time, capturing the impact of natural endowment as well as farmers' adaptation to climate changes. Interestingly, while the effect of the beneficial temperature reflected in GDD is stable over the sample period, except being much smaller in the late 1970s (P2), the effect of harmful temperature doubles in the more recent period (P4; 2017-2021) after declining from a relatively higher level in the 1950s (P1) to much lower levels in the 1970s and 1990s (P2 and P3). The positive effect of precipitation on yield intensifies in the middle period, 1975-2001 (P2-P3), but drops to the level of 1950s (P1) in the period of 2017-2021 (P4). The proportion of yield variation explained by weather conditions drops from 40% in P1 to 11%-18% in later periods.

The resulting surface plots, contour plots, and ergodic distribution plots are presented in Figures A1, A2, and A3, respectively. In Figures 6, we display the end-year yields predicted by the unconditional (in red) and conditional (in blue) transition kernels on top of the unconditional contours. The comparison between the unconditional and conditional end-year predictions illustrates the effect of changes in climate conditions over 20-year period on corn yield distribution. In general, climate change depresses yields in counties both below and significantly higher than the national average. Its effect on upper part of the distribution is more pronounced, especially in the early period of 1955-1975 (P1; panel a), but decreases over time, likely due to technological and management adaptations in more recent periods. Conversely,

[7]The data is available for download at: https://www.ncei.noaa.gov/pub/data/ghcn/daily.

the climate change impact on the lower part of the yield distribution is negative and noticeable in 1950s-1970s (panel a), but almost disappears in the 1970s-1990s (panel b) and flips to small positive effect in the transition between the 1990s and late 2000s (panel c). All these lead to increasing yield convergence to the national average across the country, especially for the counties with above average yields initially.

Figure 7 presents both unconditional (dashed curves) and conditional (solid curves) distributions of relative yields in the start year (lighter) and ergodic year (darker). Comparing the unconditional and conditional distributions illustrates that: (i) The impact of climate change on the start-year and ergodic yield distribution varies over individual sub-periods, with a relatively larger impact in the earlier periods of P1-P2 and P2-P3 (panels a and b) than in P3-P4 (panel c). (ii) Climate changes result in higher peaks, indicating an increased probability of counties achieving the national average yield, once again suggesting the convergence of county yields. (iii) Comparing the unconditional (darker dashed curve) and conditional (darker solid curve) ergodic distribution indicates that climate changes lead to a thinning of both the upper and lower tails, especially in the period of 1950s-1970s (panel a).

Next, we examine how climate change affects the distribution dynamics of per-acre farm income, comprising crop revenue and indemnity payments. We begin by conducting a regression of farm income on the three weather variables—GDD, ODD, and precipitation. We then estimate the transition kernel based on the regression residuals after adding back the estimated intercept. As discussed earlier, our focus is on the period from 1997 to 2021 (P3-P4), and the estimation results are reported in the lower panel of Table 2. While precipitation shows no significant effect, the estimated coefficients on GDD and ODD have opposite signs compared to those in the yield regression reported in the upper panel. This suggests that indemnity payments dominate per-acre income at the county level.

The means of the end-year incomes predicted by the unconditional (in red) and conditional (in blue) transition kernels are presented, along with the contour plot of the unconditional kernel, in the panel (a) of Figure 8. A comparison between the two illustrates that the primary effect of climate change is to reduce the incomes of counties at the upper part of the distribution, with more significant impacts on the higher portion. This leads to income convergence toward the national average. Panel (b) of Figure 8 plots the unconditional (dashed curves) and

conditional (solid curves) distributions of the start and ergodic years. The main differences between the two sets of distributions are evident in both the left tail and the mean. Unfavorable weather changes trigger indemnity payments to counties with poorer production conditions, increasing their total income and thus eliminating the lower-left tail of the income distribution, contributing to income convergence. On the other hand, climate change shifts down the level and probability of the mean income, spreading income more towards the right tail.

5 Conclusion

By scaling historical county-level corn yields with the national average, we investigate the dynamics of their distribution and convergence over time. The analysis aims to understand distribution changes and transitions across four subperiods with 20-year intervals, 1955-1959 (P1), 1975-1979 (p2), 1997-2001 (P3), and 2017-2021 (P4). Stochastic transition kernels illustrate the convergence of yield toward the national average over time, confirming the trend indicated by preliminary analyses of box plots and transition matrices. To identify the impact of climate change on yield distribution, conditional transition kernels are estimated using regression residuals of yields on growing degree days, overheating degree days, and precipitation. A comparison between unconditional and conditional kernels reveal that climate change more significantly reduces yields in the upper part of the distribution than in the lower part, leading to yield convergence across the country. The distribution of per-acre crop income, including crop revenue and indemnity payments, also exhibits convergence over time. However, climate change affects income distribution in more complex ways compared to yield distribution.

We conclude by highlighting a few directions for future research. First, similar empirical methods can be applied to farm-level yield records and other crops to understand their distribution dynamics and convergence of yields over time. Second, the method can be further extend to quantify changes related to specific aspects of yield distribution, such as the left and right tails. This extension would be valuable in understanding changes in systemic risks driven by fundamental factors like weather. Finally, empirical methods commonly used in the growth-convergence literature (e.g., Barnwal and Kotani, 2013; Higgins et al., 2006) can be explored to validate the results in our study and gain additional insights.

References

Antle, J. M. (1983). Testing the Stochastic Structure of Production: A Flexible Moment-Based Approach. *Journal of Business and Economic Statistis 1*(3), 192–201.

Antle, J. M. (2010). Asymmetry, Partial Moments, and Produciton Risk. *American Journal of Agricultural Economics 92*(5), 1294–1309.

Barnwal, P. and K. Kotani (2013). Climatic Impacts across Agricultural Crop Yield Distributions: An Application of Quantile Regression on Rice Crops in Andhra Pradesh, India. *Ecological Economics 87*, 95–109.

Chavas, J.-P., S. D. Falco, F. Adinolfi, and F. Capitanio (2019). Weather effects and their Long-Term Impact on the Distribution of Agricultural Yields: Evidence from Italy. *European Review of Agricultural Economics 46*(1), 29–51.

Chavas, J.-P. and G. Shi (2015). An Economic Analysis of Risk, Management, and Agricultural Technology. *Journal of Agricultural and Resource Economics 40*(1).

Du, X., D. A. Hennessy, and C. Yu (2012). Testing Day's Conjecture that More Nitrogen Decreases Crop Yield Skewness. *American Journal of Agricultural Economics 94*(1), 225–237.

Du, X. D., C. Yu, D. A. Hennessy, and R. Miao (2015). Geography of Crop Yield Skewness. *Agricultural Economics 46*, 463–473.

Falco, S. D. and J.-P. Chavas (2008). Rainfall Shocks, Resilience, and the Effects of Crop Biodiversity on Agroecosystem Productivity. *Land Economcis 84*(1), 83–96.

Gong, X., D. A. Hennessy, and H. Feng (2023). Systemic Risk, Relative Subsidy Rates, and Area Yield Insurance Choice. *American Journal of Agricultural Economics 105*, 888–913.

Goodwin, B. and A. Ker (1998). Nonparametric Estimation of Crop Yield Distributions: Implications for Rating Group Risk (GRP) Crop Insurance Contracts. *American Journal of Agricultural Economics 80*, 139–153.

Goodwin, B. K. (2001). Problems with Market Insurance in Agriculture. *American Journal of Agricultural Economics 83*(3), 643–649.

Griliches, Z. (1957). Hybrid corn: An exploration in the economics of technological change. *Econometrica 25*(4), 501.

Higgins, M. J., D. Levy, and A. T. Young (2006). Growth and Convergence across the United States: Evidence from County-Level Data. *Review of Economics and Statistics 88*(4), 671–681.

Ker, A. P. and K. Coble (2003). Model Conditinal Yield Densities. *American Journal of Agricultural Economics 85*(2), 291–304.

Ker, A. P. and B. K. Goodwin (2000). Nonparametric Estimation of Crop Insurance Rates Revisited. *American Journal of Agricultural Economics 83*(2), 463–478.

Lusk, J. L., J. Tack, and N. P. Hendricks (2019). *Heterogeneous Yield Impacts from Adoption of Genetically Engineered Corn and the Importance of Controlling for Weather*, pp. 11–39. University of Chicago Press.

Nelson, C. H. and P. Preckel (1989). The Conditinal Beta Distribution As a Stochastic Production Function. *American Journal of Agricultural Economics 71*(2), 370–378.

Park, S. and D. Shin (2023). Recent Changes in the Nature of the Distribution Dynamics of the US County Incomes. *Journal of Applied Econometrics*, forthcoming.

Quah, D. (1993). Empirical Cross-Section Dynamics in Economci Growth. *European Economic Review 37*, 426–434.

Quah, D. T. (1996a). Convergence empirics across economies with (some) capital mobility. *Journal of Economic Growth 1*(1), 95–124.

Quah, D. T. (1996b). Empirics for economic growth and convergence. *European Economic Review 40*(6), 1353–1375.

Quah, D. T. (1997). Empirics for Growth and Distribution: Stratification, Polarization, and Convergence Clubs. *Journal of Economic Growth 2*.

Ramirez, O. (1997). Estimation and Use of a Multivariate Parametric Model for Simulating Heteroscedsatic, Correlated, Non-Normal Random Variables: The Case of Corn Belt Corn, Soybean and Wheat Yields. *American Journal of Agricultural Economics 79*, 291–305.

Ramsey, A. F. (2023). Probability Distribution of Crop Yields: A Bayesian Spatial Quantile Regression Approach. *American Journal of Agricultural Economics 102*(1), 220–239.

Sanglestsawai, S., R. M. Rejesus, and J. M. Yorobe (2014). Do Lower Yielding Farmers Benefit from Bt Corn? Evidence from Instrumental Variable Quantile Regressions. *Food Policy 44*, 285–296.

Schlenker, W. and M. J. Roberts (2009). Nonlinear Temperature Effects Indicate Severe Damages to U.S. Crop Yields under Climate Change. *Proceedings of the National Academy of Science 106*(37), 888–913.

Shi, G., J.-P. Chavas, and J. Lauer (2013). Commercialized Transgenic Traits, Maize Productivity and Yield Risk. *Nature Biotechnology 31*, 111–114.

Tack, J. B. and M. T. Holt (2016). The Influence of Weather Extremes on the Spatial Correlation of Corn Yields. *Climatic Change 134*, 299–309.

Tolhurst, T. N. and A. P. Ker (2015). On Technological Change in Crop Yields. *American Journal of Agricultural Economics 97*(1), 137–158.

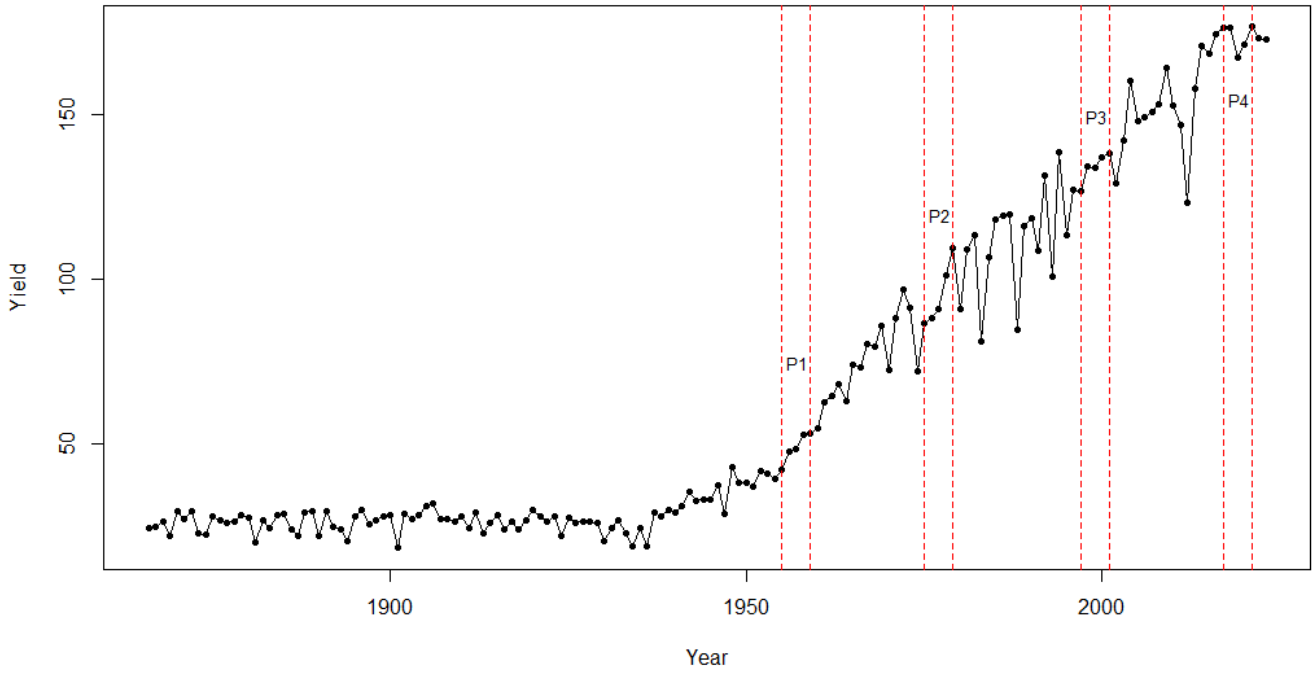

Figure 1: Sample Periods for Distribution Dynamics.

Note: The figure shows the national average yields from 1886 to 2023 obtained from the NASS database. The subperiods marked by the vertical lines are as follows: P1 (1955-1959), P2 (1975-1979), P3 (1997-2001), and P4 (2017-2021).

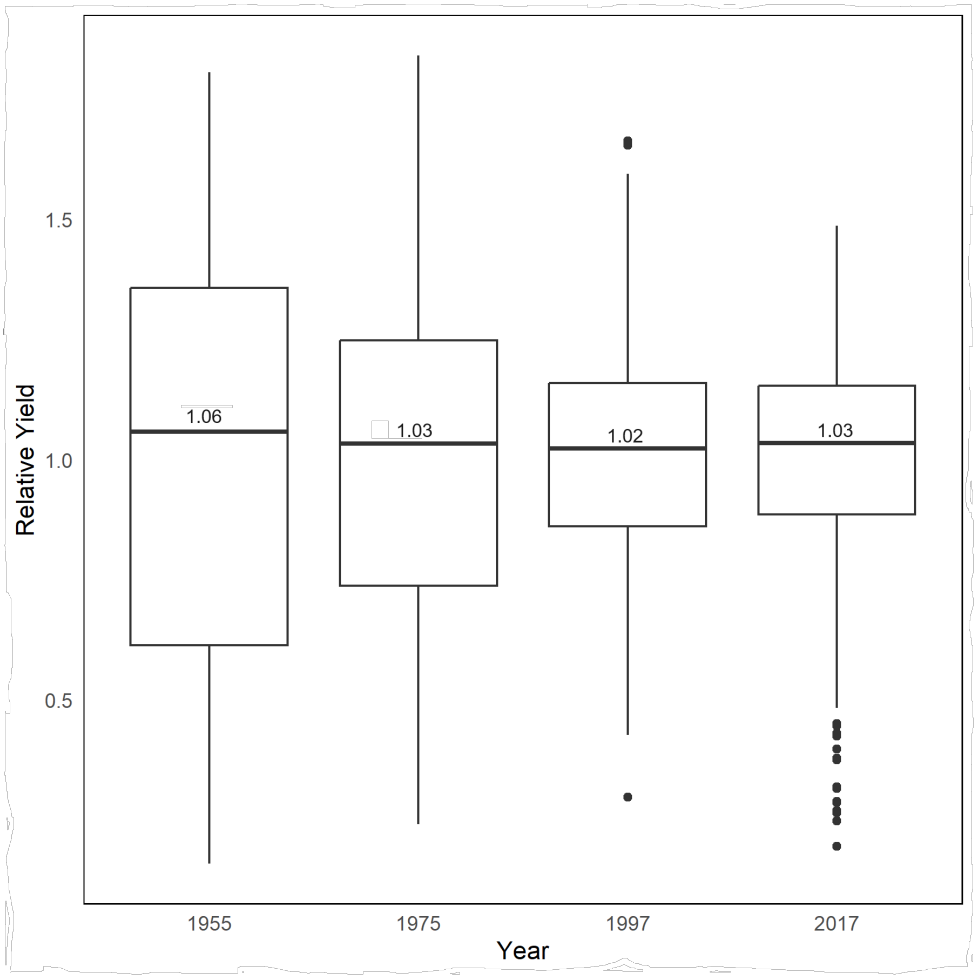

Figure 2: Boxplots of Relative County Yields.

Note: The number on the horizontal bar represents the median value of relative yields for each sample year.

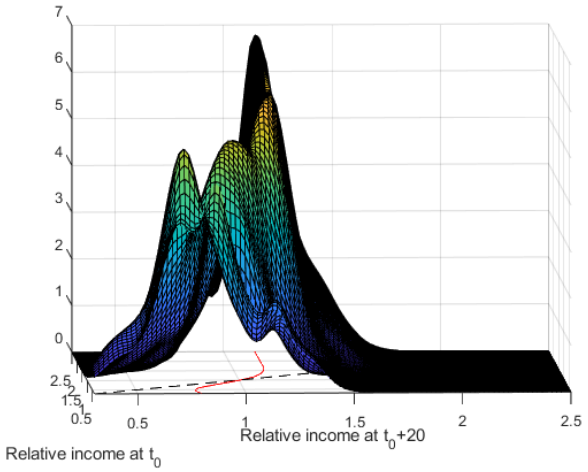

(a)

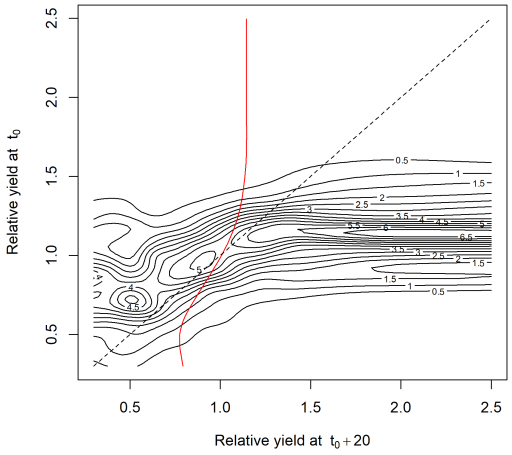

(b)

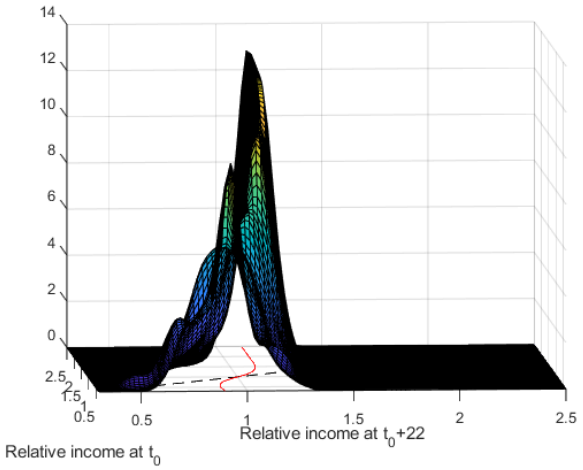

(c)

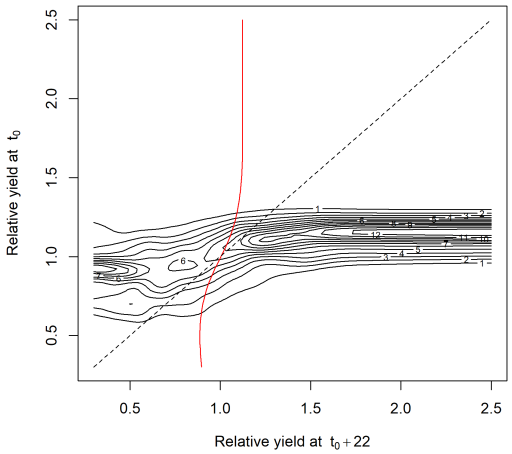

(d)

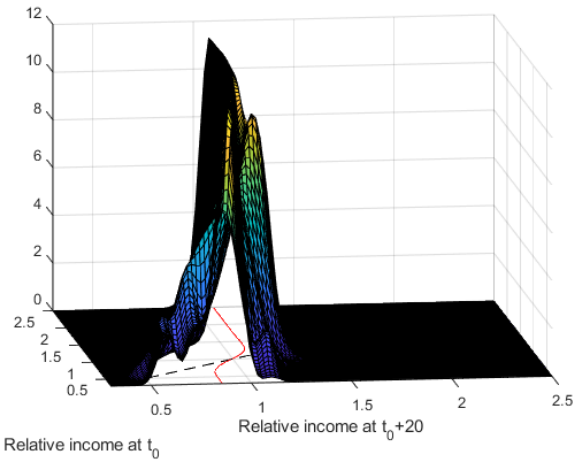

(e)

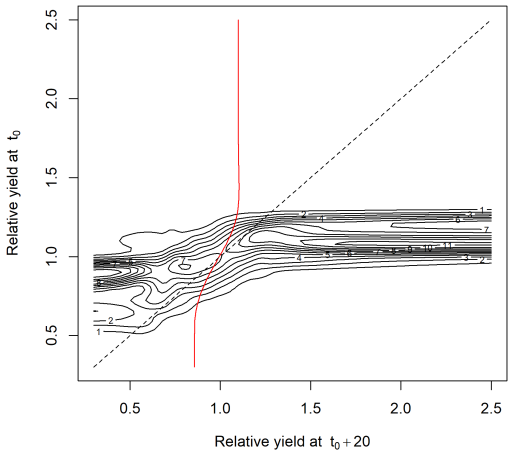

(f)

Figure 3: Surface and Contour Plots of Sub-Periods (Unconditional).

Note: (a)/(b) P1-P2; (c)/(d) P2-P3; (e)/(f) P3-P4.

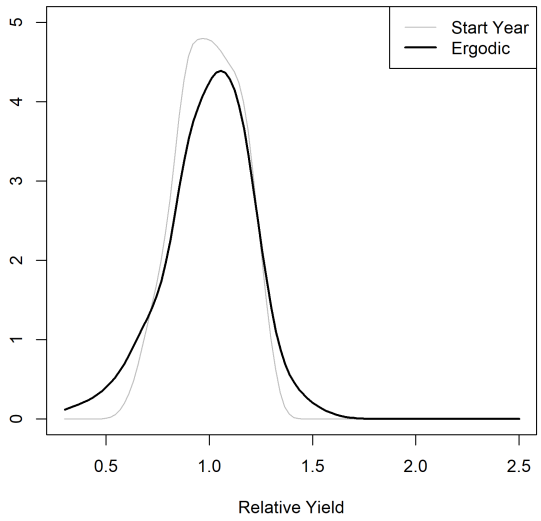

(a)

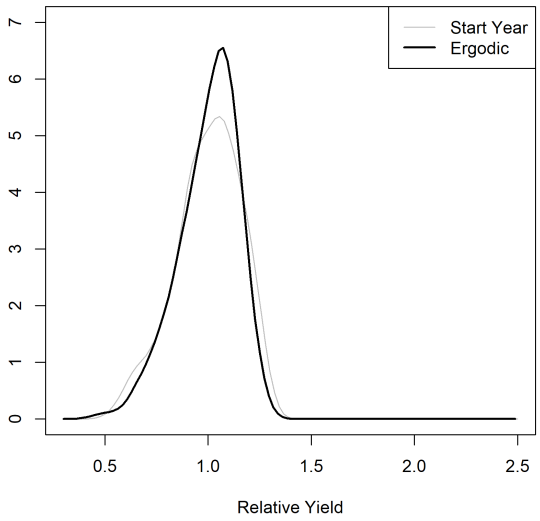

(b)

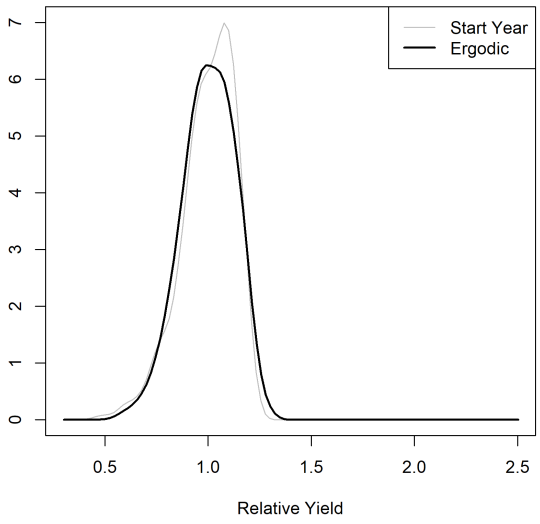

(c)

Figure 4: Ergodic Distributions of Sub-Periods (Unconditional).

Note: (a) P1-P2; (b) P2-P3; (c) P3-P4.

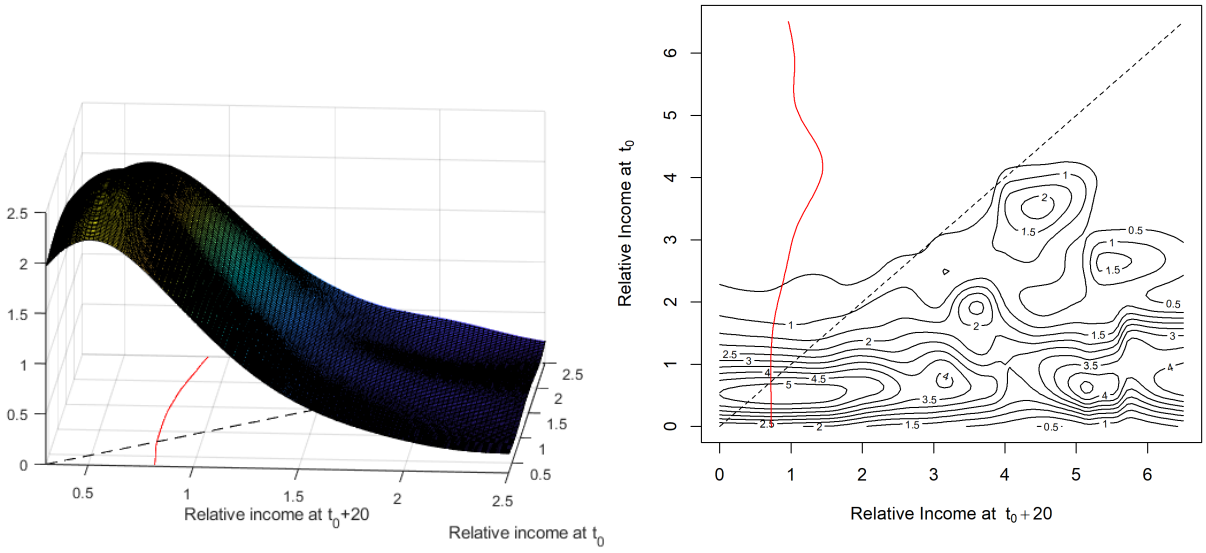

(a) (b)

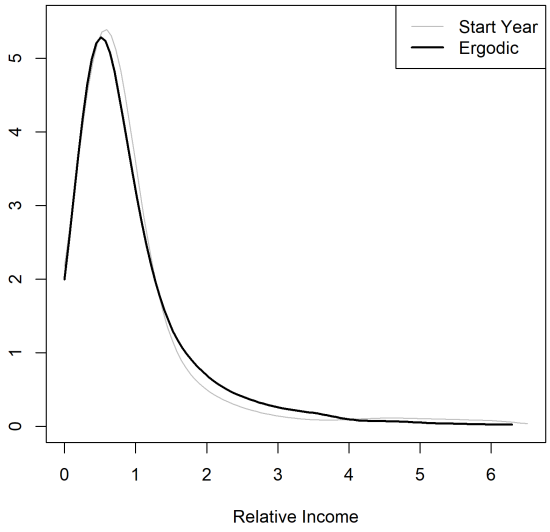

(c)

Figure 5: Distribution Dynamics of Relative Crop Income over P3-P4.

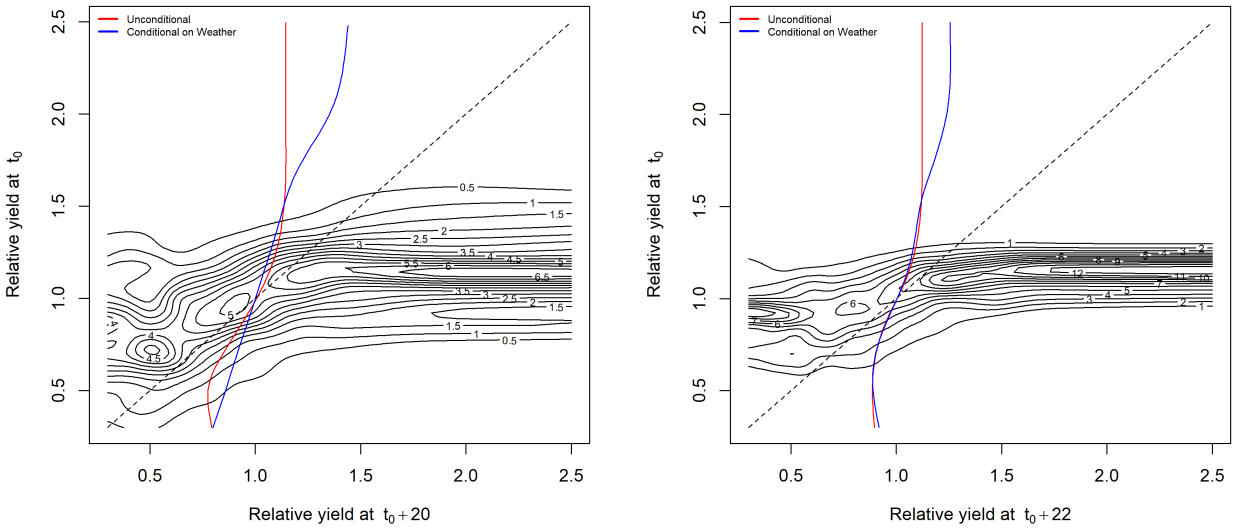

(a)

(b)

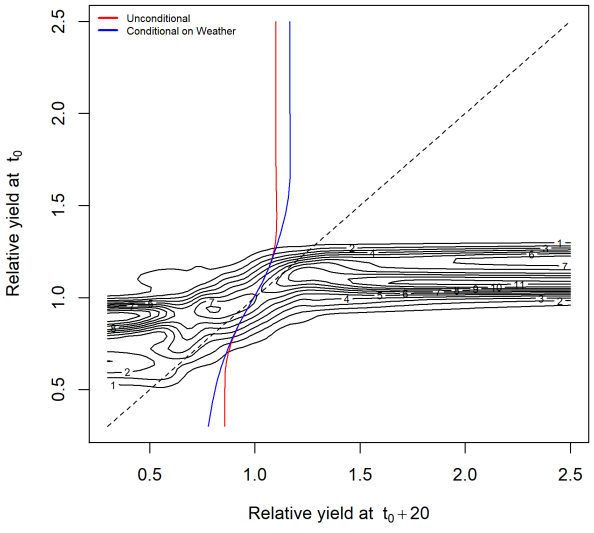

(c)

Figure 6: Contour Plots of Sub-Periods (Unconditional and Conditional on weather variables).

Note: (a) P1-P2; (b) P2-P3; (c) P3-P4.

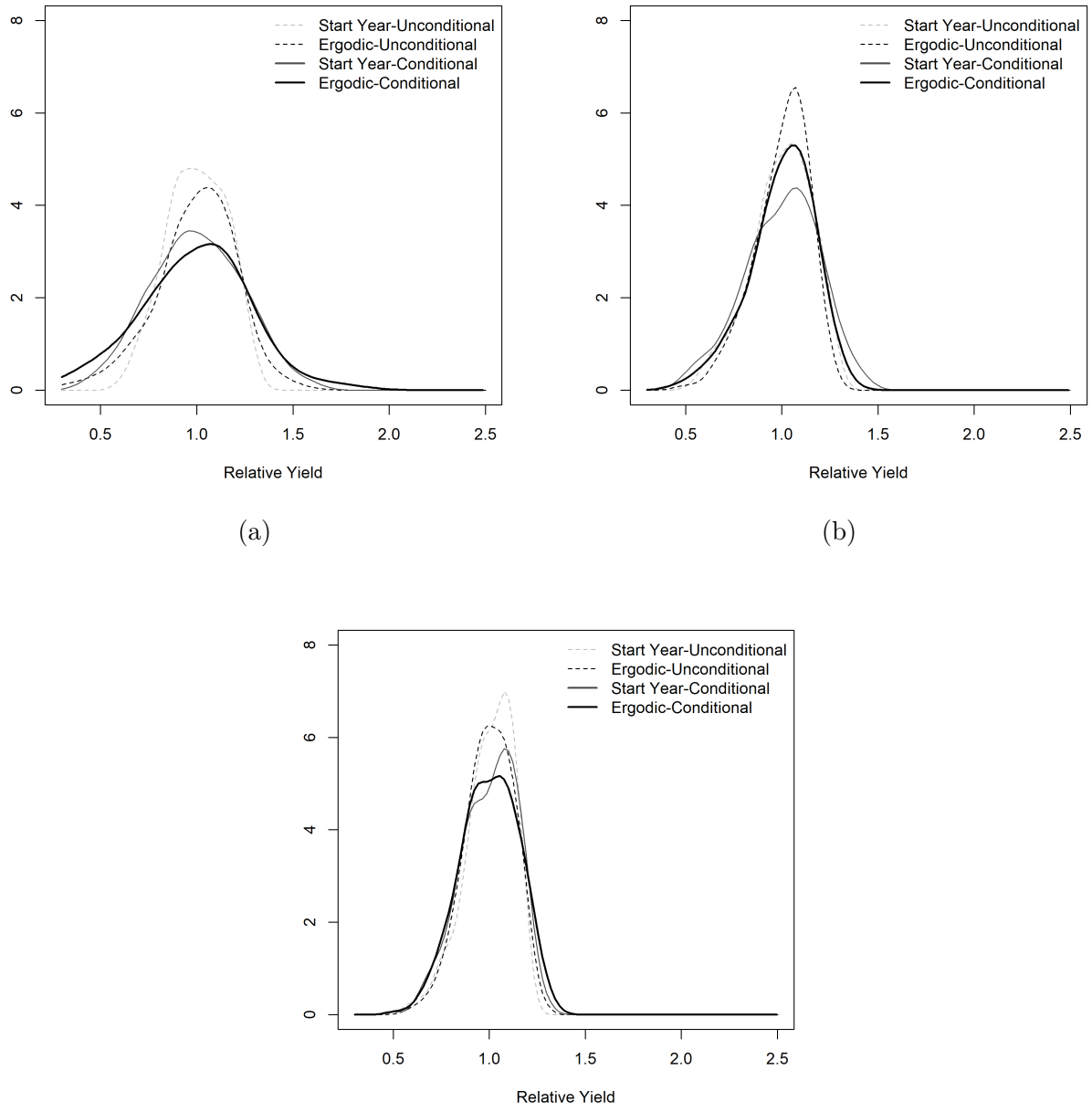

(a) (b)

(c)

Figure 7: Ergodic Distributions of Subperiods (Unconditional and Conditional).

Note: (a) P1-P2; (b) P2-P3; (c) P3-P4.

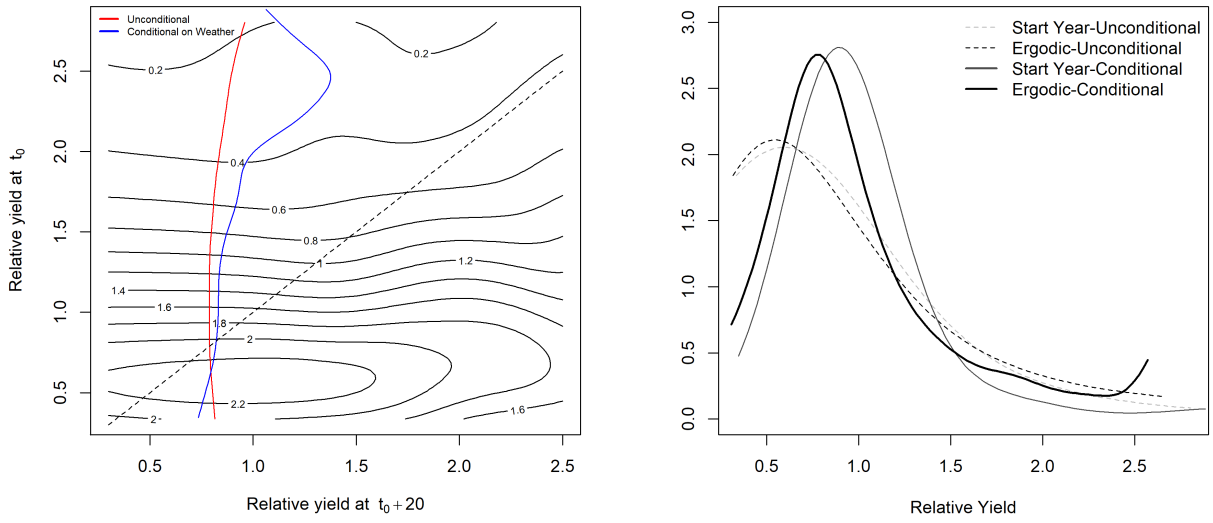

(a) (b)

Figure 8: Distribution Dynamics of Relative Crop Income Conditional on Weather over P3-P4.

Table 1: Transition Matrix Between Sub-Periods.

	[0,0.5]	[0.5,0.75]	[0.75,1]	[1,1.25]	[1.25,2]
P1 – P2					
1	0.28	0.30	0.18	0.15	0.09
2	0.18	0.28	0.30	0.17	0.07
3	0.07	0.21	0.35	0.29	0.09
4	0.02	0.09	0.28	0.43	0.18
5	0.01	0.02	0.11	0.40	0.46
P2 – P3					
1	0.13	0.43	0.33	0.10	0.01
2	0.04	0.25	0.51	0.18	0.02
3	0.02	0.15	0.44	0.36	0.04
4	0.003	0.06	0.26	0.56	0.12
5	0.001	0.01	0.11	0.64	0.24
P3 – P4					
1	0.37	0.41	0.22	0	0
2	0.11	0.37	0.43	0.08	0.003
3	0.03	0.13	0.44	0.39	0.01
4	0.003	0.03	0.19	0.64	0.14
5	0	0.03	0.12	0.61	0.23

Note: The table reports the average transition probabilities among five ranges of relative county corn yields compared to the national average during four sub-periods, P1 (1955-1959), P2 (1975-1979), P3 (1997-2001), and P4 (2017-2021). The ranges are as follows: 1-[0,0.5], 2-[0.5,0.75], 3-[0.75,1], 4-[1,1.25], and 5-[1.25,2]. The averages are based on five pairs of start and end years, for example, 1955 and 1975, 1956 and 1976, 1957 and 1977, 1958 and 1978, and 1959 and 1979 for the transitions between P1 and P2.

Table 2: OLS Regression Results of Weather Variables

Variables	P1	P2	P3	P4
Relative Yield				
Intercept	9.10***	55.24***	87.44***	129.63***
	(1.44)	(2.50)	(2.76)	(3.63)
GDD	0.03***	0.007***	0.02***	0.03***
	(0.001)	(0.002)	(0.002)	(0.003)
ODD	-0.32***	-0.13***	-0.17***	-0.73***
	(0.007)	(0.01)	(0.01)	(0.03)
Precipitation	0.01***	0.06***	0.05***	0.01***
	(0.002)	(0.004)	(0.004)	(0.005)
R^2	0.40	0.12	0.11	0.18
Relative Farm Income				
Intercept			6538.62***	
			(1053.07)	
GDD			-3.16***	
			(0.86)	
ODD			39.80***	
			(10.30)	
Precipitation			1.39	
			(1.24)	
R^2			0.01	

Note: Standard errors are enclosed in parentheses. Significance levels are denoted as ***, **, and *, representing 1%, 5%, and 10% significance, respectively.

Appendix

Appendix A Figures and Tables

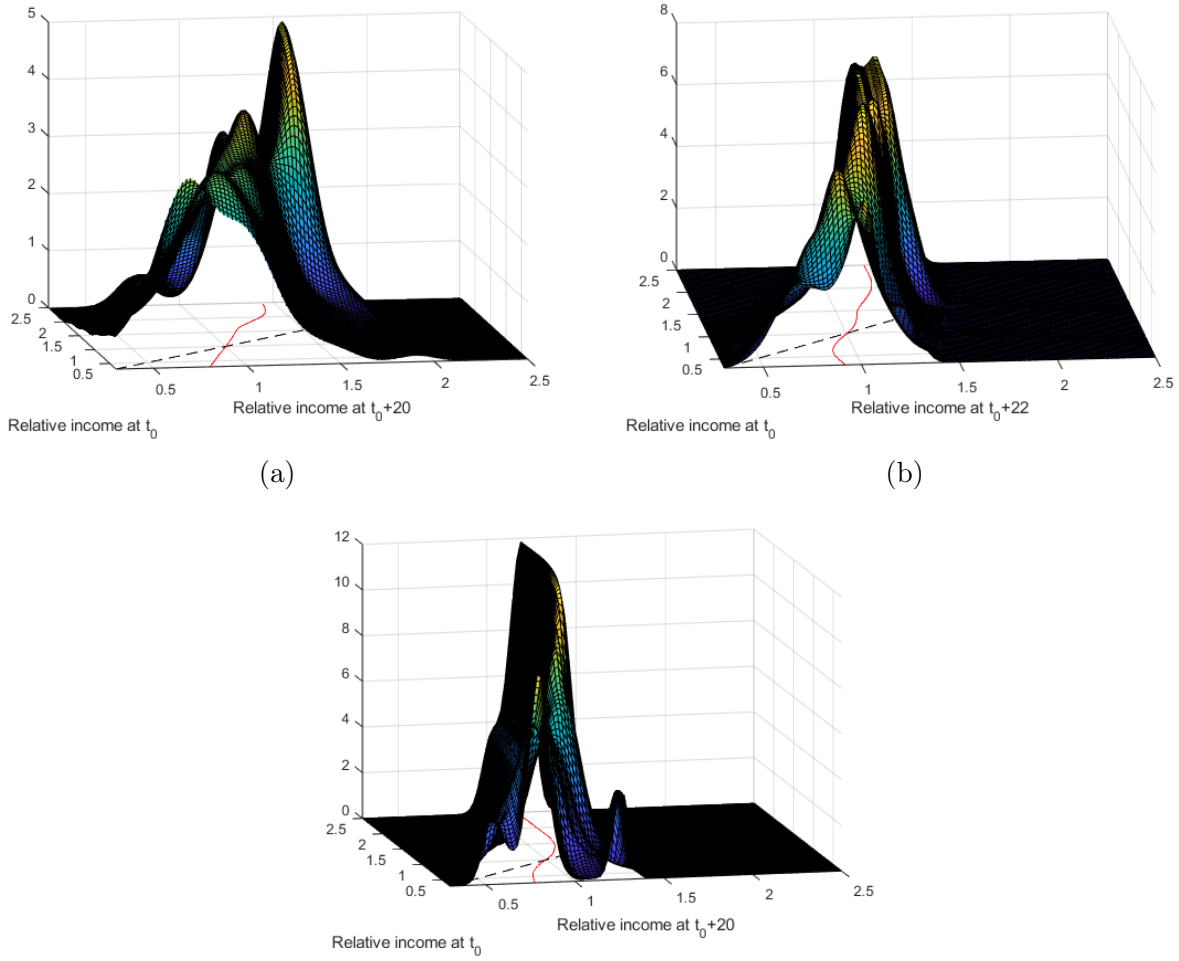

(a) (b)

(c)

Figure A1: Surface Plots of Sub-Periods (Conditional on weather variables).

Note: (a) P1-P2; (b) P2-P3; (c) P3-P4.

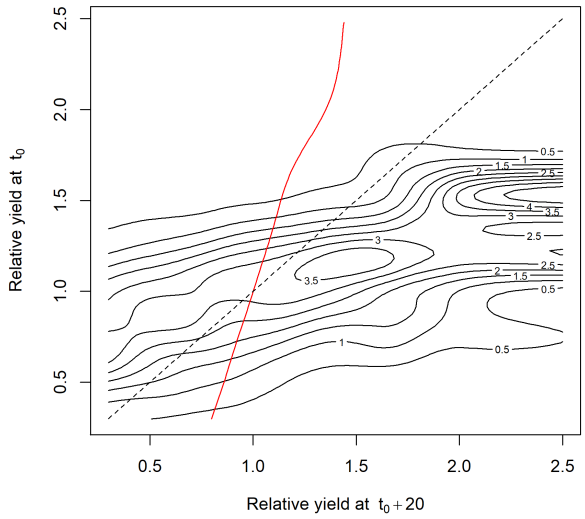

(a)

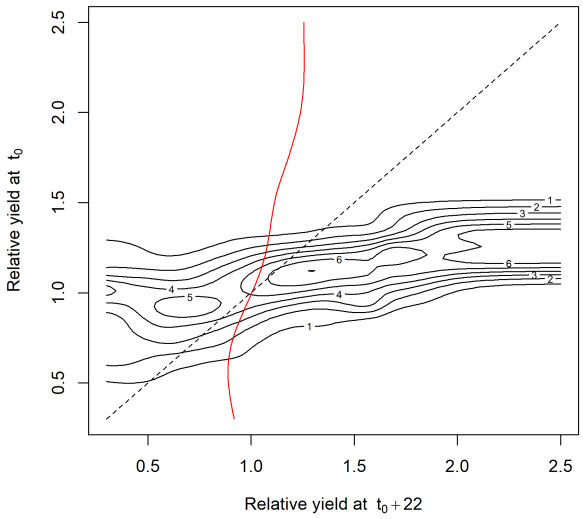

(b)

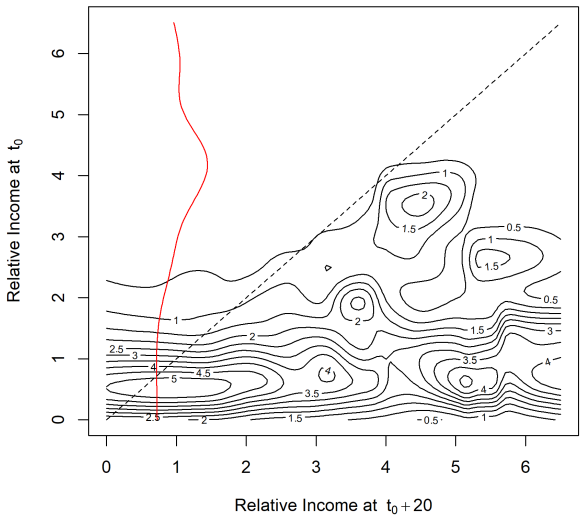

(c)

Figure A2: Contour Plots of Sub-Periods (Conditional on weather variables).

Note: (a) P1-P2; (b) P2-P3; (c) P3-P4.

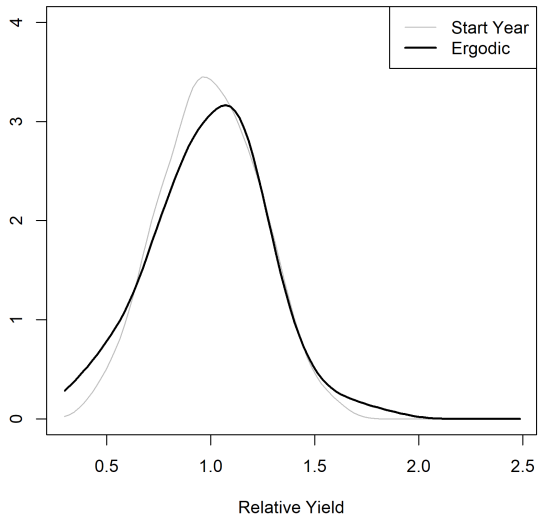

(a)

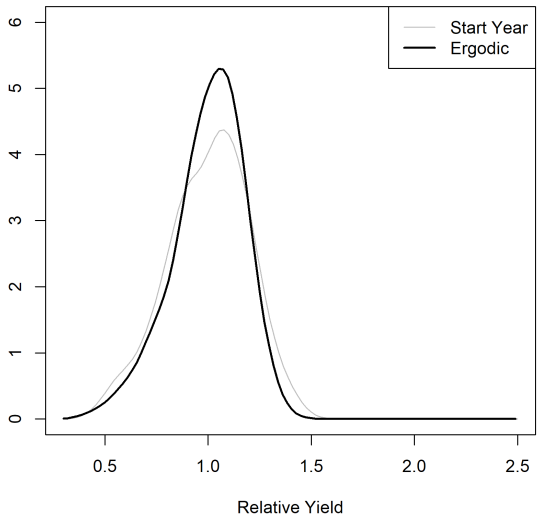

(b)

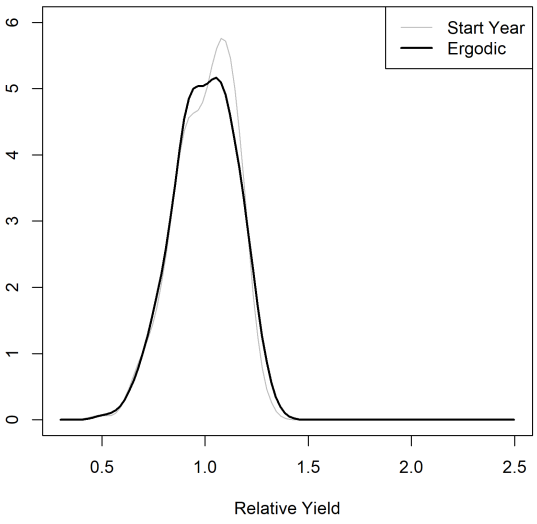

(c)

Figure A3: Ergodic Distribution of Sub-Periods (Conditional on weather variables).

Note: (a) P1-P2; (b) P2-P3; (c) P3-P4.